Apathy progression is associated with brain atrophy and white matter damage in Parkinson's disease

Roqaie Moqadam[1,2,3], Houman Azizi[2,4,5], Aliza Brzezinski-Rittner[2,5,7] Lucas Ronat[1,3], Alexandru Hanganu[3,6], Yashar Zeighami[2,7,†], Mahsa Dadar[2,7,†]

1. Department of Medicine, University of Montreal, Montreal, Quebec, Canada
2. Douglas Mental Health University Institute, Montreal, Quebec, Canada
3. Centre de Recherche, Institut Universitaire de Gériatrie de Montréal, Québec, Canada
4. Montreal Neurological Institute and Hospital, McGill University, Montreal, Quebec, Canada
5. Integrated Program in Neuroscience, McGill University, Montreal, Quebec, Canada
6. Department of Psychology, University of Montreal, Montreal, Quebec, Canada
7. Department of Psychiatry, McGill University, Montreal, Quebec, Canada

[†] These authors contributed equally to this work.

Correspondence to:

Mahsa Dadar, Douglas Mental Health University Institute, Montreal, Quebec, Canada
Roqaie Moqadam, Douglas Mental Health University Institute, Montreal, Quebec, Canada
Emails:mahsa.dadar@mcgill.ca, roqaie.moqadam@umontreal.ca

Abstract

Apathy is a prevalent non-motor symptom that significantly impacts the quality of life in Parkinson's disease (PD) patients. Although previous studies have investigated the neural correlates of apathy in PD, the longitudinal relationships between regional brain atrophy, white matter hyperintensities (WMHs), and apathy progression remain underexplored. Using longitudinal, multisite data of *de novo* PD patients from the Parkinson's Progression Markers Initiative (PPMI), the present study aims to investigate these relationships.

We used T1-weighted magnetic resonance imaging (MRI) and clinical data from 445 participants. Apathy was assessed as part of the Movement Disorder Society Unified Parkinson's Disease Rating Scale (MDS-UPDRS) Part I. We applied deformation-based morphometry (DBM) to quantify gray matter atrophy and used the Brain tISsue segmentatiON (BISON) algorithm to segment WMHs from T1-weighted images. Using linear regression models, we performed cross-sectional analyses to identify the associations between baseline brain measurements (DBM and WMH) and apathy severity. Longitudinal analyses utilized linear mixed-effects models to investigate whether baseline brain measurements were associated with future apathy progression over time, accounting for covariates such as age, sex, motion artifacts, Hoehn and Yahr stage, levodopa-equivalent daily dose (LEDD), Total Intracranial Volume (TIV), and baseline apathy. Hypothesis-based and exploratory analyses were conducted to confirm the results previously reported in the literature and explore potential new associations.

No cross-sectional regional associations survived multiple comparison corrections. Longitudinal hypothesis-based models confirmed that baseline atrophy in regions such as the bilateral nucleus accumbens area, superior parietal, putamen, insula, left precuneus, right precentral, and cerebellum gray matter was significantly associated with future apathy progression. Exploratory longitudinal analyses identified additional regions, including the bilateral lingual, parahippocampal, basal forebrain, ventral diencephalon, isthmus cingulate, thalamus, hippocampus, left middle temporal, right inferior temporal, pericalcarine, medial orbitofrontal, cuneus, where baseline atrophy was correlated with progression of apathy severity. Moreover, greater WMH burden, particularly in the frontal lobe, was associated with worsening apathy. These results highlight the influence of both gray matter atrophy and WMHs on apathy progression in PD.

Keywords: Parkinson's disease; apathy; magnetic resonance imaging; deformation-based morphometry; white matter hyperintensities; longitudinal analysis

Introduction

Parkinson's disease (PD) is the second most common neurodegenerative disorder after Alzheimer's disease. In addition to its well-known motor symptoms including tremors, bradykinesia, rigidity, and postural instability, PD is associated with a range of non-motor symptoms such as apathy, depression, anxiety, cognitive impairment, sleep disturbances, and autonomic dysfunction[1,2]. Characterized by a lack of motivation, interest, and emotional engagement, apathy is one of the common neuropsychiatric symptoms in PD, substantially impacting the quality of life and independence of the patients[2–5].

Stuss and colleagues define three distinct subtypes of apathy, including behavioral, motivational, and cognitive apathy, each associated with specific neural circuits[6–8]. While apathy is also present in up to 30% of healthy older adults, the apathy observed in PD patients is believed to differ from that associated with healthy aging[6,9]. This difference is primarily due to its association with specific neurotransmitter dysfunctions and alterations in apathetic PD patients[10]. As such, PD apathy is associated with dopaminergic deficits and disruptions in fronto-striatal circuits. These dysfunctions negatively impact reward processing, intrinsic motivation, and emotion regulation[6,10,11]. Structural changes in areas such as the basal ganglia and frontal cortex are thought to contribute to these deficits, emphasizing how PD-related apathy might differ from the aging-related alterations in motivation and engagement[6].

The literature reports varying results in the prevalence of apathy across different PD populations, with a wide range from 13.9% to 70% depending on different factors including demographics, diagnostic criteria and assessment tools, disease stage, and treatment[3,4,12]. While apathy can emerge at any stage of the disease, it is frequently present in earlier disease stages[6]. In a recent review of the non-motor aspects of PD symptomatology, apathy was recognized as a distinct feature, occurring several years before the motor symptoms became evident[2]. In a cohort of 109 newly diagnosed untreated PD patients, apathy was commonly reported during the two-year period preceding the motor symptoms, with approximately 11% of the cohort identifying its onset within the period preceding the motor symptoms[13].

Previous neuroimaging studies in cross-sectional samples have reported associations between cortical and subcortical atrophy and apathy in PD patients[14–23]. These studies vary in their approach to evaluating apathy, using either presence or severity measures. Regarding presence of apathy, several studies used the Neuropsychiatric Inventory (NPI)[24] and Lille Apathy Rating Scale (LARS)[25] to identify brain regions associated with apathy. These studies consistently reported associations between apathy presence and atrophy in regions such as the anterior cingulate cortex, nucleus accumbens, and caudate, emphasizing the involvement of frontostriatal circuits in presence of apathy[15–21]. Studies focusing on apathy severity often utilize the Starkstein Apathy Scale (SAS)[26], Apathy Evaluation Scale (AES-I)[14,27], and NPI. These studies established correlations between the severity of apathy and atrophy in certain brain regions including the inferior parietal lobule, orbitofrontal cortex, and insula, underscoring the relationship between cortical degeneration and apathy severity[14,15,19,20,22,23] (Table 1). Longitudinal assessments of

apathy related to brain atrophy have been more scarce. Morris et al[21]. reported an association between the nucleus accumbens volume and the presence of apathy over 2 years of follow-up. In contrast, Ranjbar et al[23]. reported a correlation between lower atrophy in the right putamen and increased apathy severity over time.

Beyond associations with gray matter atrophy, apathy has been linked to spatially extensive reductions in white matter (WM) integrity[28]. Using diffusion-weighted imaging (DWI), Wen et al[29]. found a decrease in WM network efficiency and connectivity related to apathy in PD, particularly within the frontal, temporal, parietal, and basal ganglia regions. However, DWI is not frequently used clinically, particularly in the context of PD[30]. On the other hand, in normal aging and individuals with Alzheimer's disease[28,31], the literature reports significant associations between apathy symptoms and increased volume of white matter hyperintensities (WMHs) in frontal and temporal lobes, areas critical for motivation and emotional regulation[28]. WMHs are areas of increased signal on fluid-attenuated inversion recovery (FLAIR) sequences and are markers of cerebrovascular pathology[32]. WMHs are also commonly present in patients with PD[33]. The association between WMHs and apathy in PD remains understudied, with a single study in a cohort of 141 PD patients reporting a significant link between WMH and apathy, where WMH severity was a strong predictor of apathy severity and progression in the patients[30]. However, this study used visual Fazekas scale for WMH assessment[34], which does not reflect the full extent of WMH burden. In addition, only global WMH rating was utilized and the study did not assess how WMHs in different brain regions contribute to apathy[30].

Although neural correlates of apathy have previously been examined, longitudinal relationships between regional cerebral atrophy, WMHs, and apathy require further investigation. The present study takes advantage of the large sample size and the availability of longitudinal clinical data from the Parkinson's Progression Markers Initiative (PPMI) dataset to examine the relationship between apathy, regional brain atrophy, and WMH in patients with PD. We hypothesize that regional brain atrophy and WMH are associated with the severity and future progression of apathy in PD patients.

Table 1. Regions linked to apathy in PD based on previous literature.

Region Name	References	Sample size (disease stage)	Apathy Assessment	Presence /Severity	Covariates
Middle Frontal	Alzahrani et al.[16]	65 (Mild)	NPI	Presence	Age, Education, Sex, TIV
	Rashidi-Ranjba et al.[23]	137 (Early to moderate, MoCA > 19)	NPI	Severity	Age, Sex, Education
Nucleus Accumbens	Morris et al.[21]	199 (HY~ 1-3)	NPI	Presence	Age, Sex, UPDRS-III, MoCA
	Carriere et al.[15]	20 (non-demented, non-depressed)	LARS	Severity	LEDD, DD
	Martinez-Horta et al.[17]	36 (Early to mid, HY: 1.8 ± 0.4)	UPDRS-I	Presence	Age, Sex, TIV
Lateral Orbitofrontal	Martinez-Horta et al.[17]	36 (Early to mid, HY: 1.8 ± 0.4)	UPDRS-I	Presence	
Rostral Anterior Cingulate	Alzahrani et al.[16]	65 (Mild)	NPI	Presence	
	Morris et al.[21]	199 (HY: 1-3)	NPI	Presence	
	Prange et al.[20]	27 (De novo)	LARS	Presence	Age, Sex
Superior Parietal	Martinez-Horta et al.[17]	36 (Early to mid, HY: 1.8 ± 0.4)	UPDRS-I	Presence	
Inferior Parietal	Reijnders et al.[14]	55 (H&Y: 1.5-3)	LARS	Severity	Age, MMSE, GM volume
	Martinez-Horta et al.[17]	36 (Early to mid, HY: 1.8 ± 0.4)	UPDRS-I	Presence	
Putamen	Ye et al.[19]	207 de novo ~ MCI	NPI	Presence	Age, Sex, education, TIV
Insula	Alzahrani et al.[16]	65 (Mild)	NPI	Presence	
	Reijnders et al.[14]	55 (HY: 1.5-3)	LARS	Severity	
	Ye et al.[19]	207 (de novo ~ MCI)	NPI	Presence, Severity	
	Rashidi-Ranjba et al.[23]	137(Early to moderate, MoCA > 19)	NPI	Severity	
Precuneus	Reijnders et al.[14]	55 (HY: 1.5-3)	LARS	Severity	
Precentral	Alzahrani et al.[16]	65 (Mild)	NPI	Presence	
	Reijnders et al.[14]	55 (H&Y: 1.5-3)	LARS	Severity	
Caudal Midbrain	Prange et al.[20]	27 (de novo)	SAS	Severity	
Inferior Frontal	Alzahrani et al.[16]	65 (Mild)	NPI	Presence	
	Martinez-Horta et al.[17]	36 (Early to moderate, HY: 1.8 ± 0.4)	UPDRS-I		
	Reijnders et al.[14]	55 (HY: 1.5-3)	LARS	Severity	
Superior Temporal	Alzahran et al.[16]	65 (Mild)	NPI	Presence	
	Prange et al.[20]	27 (De novo)	LARS	Presence	
	Rashidi-Ranjba et al.[23]	137 (Early to moderate, MoCA > 19)	NPI	Severity	
Cerebellum GM	Prange et al.[20]	27 (de novo)	SAS	Severity	
Caudate	Morris et al.[21]	199 (HY~ 1-3)	NPI	Presence	
	Carriere et al.[15]	20 (non-demented, non-depressed)	LARS		
No regions	Lucas□Jiménez et al.[18]	32 (HY≤ 3)	LARS	Presence	TIV, UPDRS-III, MCI
No regions	Sampedro et al.[22]	44 (DD: 9 yrs, relatively high UPDRS-III)	SAS	Severity	Age, sex, education, DD LEDD, UPDRS-III

LARS: Lille Apathy Rating Scale. SAS: Starkstein Apathy Scale. NPI: Neuropsychiatric Inventory. UPDRS: Unified Parkinson's Disease Rating Scale. DD: Disease Duration. HY: Hoehn and Yahr. TIV: Total Intracranial Volume. MCI: Mild Cognitive Impairment. LEDD: levodopa-equivalent daily dose. GM: Gray Matter. MoCA: Montreal Cognitive Assessment.

*Item 4, Apathy Score 2/3

Materials and methods

Data

T1-weighted MRI and clinical data from 546 participants with PD were obtained from the Parkinson's Progression Markers Initiative (PPMI) database (www.ppmi-info.org/data)[35]. The PPMI is a longitudinal, multi-site observational study of newly diagnosed and untreated patients with PD across the United States and Europe. Clinical assessments included Hoehn and Yahr stage (HY Stage), and apathy scores based on the Movement Disorders Society Unified Parkinson's Disease Rating Scale part I (MDS-UPDRS part I)[35,36]. Levodopa equivalent daily dosage (LEDD) was calculated based on the dosage and type of the dopaminergic medications taken at the time of the each visit according to the guidelines provided by the PPMI (https://www.ppmi-info.org/sites/default/files/docs/PPMI Data User Guide.pdf). Clinical and demographic data were organized and processed through our open source data wrangling pipeline (https://github.com/HoumanAzizi/PPMI_Data_Wrangling). Participants who had received medication at baseline, or had missing MRI, demographics, or clinical information were excluded from the present study.

MRI preprocessing

Figure 1 provides a schematic of the MRI processing steps performed. T1-weighted MRIs were processed using our open-source image processing pipeline based on the open-access MINC-Toolkit v2 (https://bic-mni.github.io/) and Advanced Normalization Tools (ANTs) (https://stnava.github.io/ANTs/) toolkits (https://github.com/VANDAlab/Preprocessing_Pipeline). Preprocessing steps included noise reduction[37], intensity non-uniformity correction[38], and intensity normalization into the range [0–100]. The preprocessed T1-weighted images were first linearly[39] and then nonlinearly[40] registered to the MNI-ICBM152 average template[41]. All the image processing steps (i.e. pre-processing, linear, and nonlinear registrations) were visually quality controlled by an experienced rater (R.M.) blind to the clinical diagnosis, and the cases that did not pass this quality control step (N = 44) were excluded from the subsequent analyses.

Deformation-based morphometry (DBM)

Deformation-based morphometry **(**DBM) was used to extract regional gray matter atrophy, calculated as the Jacobian determinant of the deformation field from the nonlinear transformations[42]. DBM values reflect the relative volume of each voxel compared to the MNI-ICBM152 template, i.e. a value of 1 denotes the same volume compared to its equivalent voxel in the template, a value below 1 denotes a smaller volume than the corresponding voxel in the template, and a value above 1 denotes larger volume than the corresponding voxel in the template. Therefore, atrophy for a particular region can be inferred from decrease in DBM values. Average gray matter atrophy in 102 cortical and subcortical regions were determined using the CerebrA atlas[41].

WMH measurements

BISON[43], a previously validated automatic segmentation tool was used to segment the WMHs. BISON combines a Random Forest classifier with a collection of location and intensity features obtained from a library of manually segmented scans to detect WMHs (Figure 1). Since the PPMI dataset lacked consistently acquired T2-weighted and Fluid attenuated inversion recovery (FLAIR) images for all participants, T1-weighted images were utilized for WMH segmentation. Although FLAIR and T2-weighted images are ideal for performing WMH assessments, in our previous work, we have shown that T1w-based segmentations from BISON yield estimates with strong correlations with FLAIR-based segmentations ($r = 0.96$)[44], and have been previously used to assess WMH burden based on T1w images in multi-center cohorts, including the PPMI[45–47]. The WMH segmentations were visually quality controlled by an experienced rater (R.M.), and cases that did not pass this quality control step ($N = 7$) were excluded from the analyses. The number of voxels designated as WMH (measured in mm^3) in the standard space (i.e. adjusted for intracranial volume) in each brain lobe and hemisphere (based on Hammer's lobar atlas[44,48]) as well as across the entire brain were used to define regional and global WMH volumes, respectively[44,49]. WMH volumes were log-transformed to obtain a normal distribution.

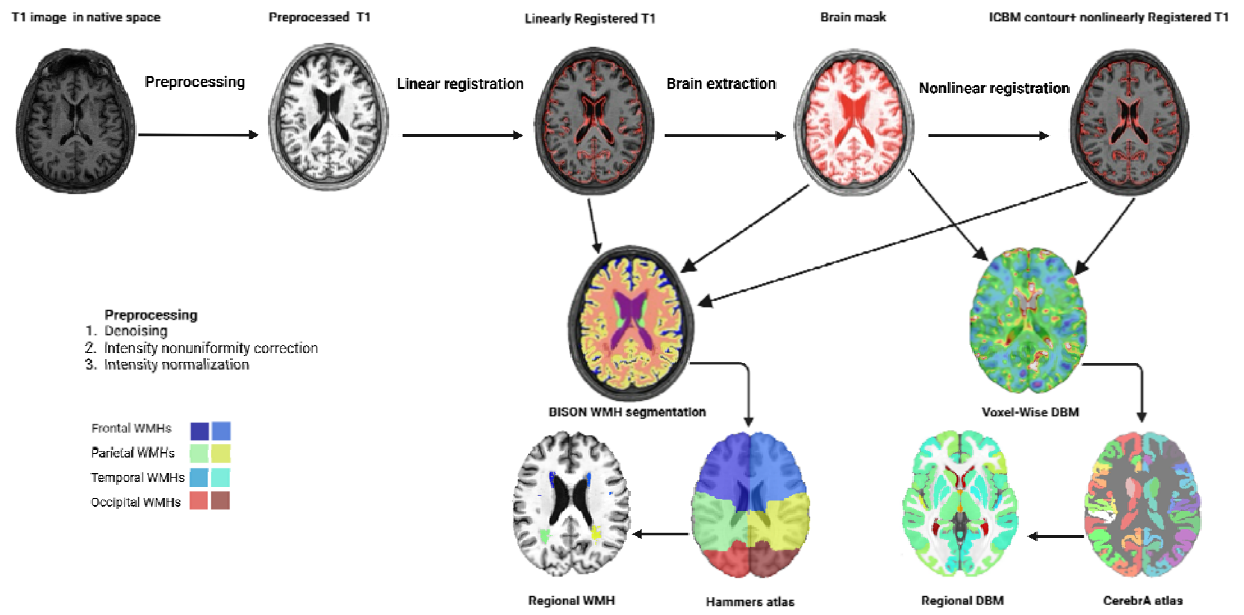

Figure 1. Flow diagram of the MRI processing steps performed. Native T1w images were preprocessed and linearly registered to the MNI-ICBM152 average template. Nonlinear registration was performed following brain extraction to derive voxel-wise DBM maps. CerebrA atlas was then used to extract regional DBM measures. The outputs of the linear registration, brain mask, and nonlinear registration steps were also used by BISON to derive voxel-wise WMH segmentations. Hammers lobar atlas was used to extract regional WMH measures. DBM: Deformation-based morphometry. WMH: White Matter Hyperintensity.

Motion assessment

Previous research including ours has shown a subtle but consistent impact of motion on gray matter atrophy estimations [50–52]. As such, all the images that passed the QC steps outlined in the previous steps further underwent a visual inspection process to assess the presence and severity of motion similar to our previous work (R.M.)[52]. Based on our previous findings, cases with motion severity ratings greater than 3 (N = 27) were excluded[52]. Motion severity scores were further used as covariates in all models[52](Figure 2).

Apathy assessment

Apathy was assessed using the Unified Parkinson's Disease Rating Scale (UPDRS) part I with the following criteria: 0 represents no apathy, 1 indicates slight apathy, when the patient experiences apathy less than one day per week, 2 denotes mild apathy, when the patient experiences apathy more than one day per week but less than half of the days, 3 indicates moderate apathy, when the patient feels apathetic more than half of the days, 4 corresponds to severe apathy where the patient feels apathetic all the time[36].

Statistical analyses

Cross-sectional analyses

The following linear regression models were used to investigate the cross-sectional relationships between brain measurements (i.e. regional DBM and WMH values) and apathy scores at baseline.

Apathy *~ Brain Measure + Age + Sex + Motion rating + TIV + HY Stage*

The variable of interest was *Brain Measure*, indicating the associations between the brain measures (i.e. regional DBM and WMHs) and apathy after accounting for covariates. Age, sex, Total Intracranial Volume (TIV)[53], motion rating, and HY Stage were included as covariates in the models.

Longitudinal analyses

A series of mixed-effect models were used to investigate the relationship between baseline brain measures and longitudinal changes in apathy scores. The following linear mixed-effects models were conducted to examine whether regional DBM, total, or regional WMH would influence the apathy score:

Apathy *~ Brain Measure Baseline + Years from Baseline + Brain Measure Baseline :Years from Baseline + Age Baseline + Sex + Motion rating Baseline +Apathy Baseline + TIV + LEDD + HY Stage +(1|Patient ID)*

The variable of interest was the interaction term *Brain Measure:Years from Baseline*, reflecting how baseline atrophy and WMHs contribute to future apathy in PD. Age at baseline, sex, motion rating (corresponding to the baseline MRI), HY Stage, baseline apathy scores, TIV, and LEDD

were included as covariates. Patient ID was included as a categorical random effect.

Hypothesis-based and exploratory analyses

The DBM analyses were performed at two levels: i) hypothesis-based, assessing the impact of atrophy in brain regions reported to be associated with apathy in PD in the literature[14–23], and ii) exploratory, assessing the potential impact of atrophy in all CerebrA GM regions to determine if any new regions could be identified. Table 1 presents the list of the regions included in the hypothesis-based analyses and whether their atrophy was related to apathy presence or severity from the literature. Similar analyses were also completed for global as well as regional WMHs. All analyses (i.e. GM and WMHs) were corrected for multiple comparisons using the False Discovery Rate (FDR) controlling technique[54]. All statistical analyses were performed using MATLAB version 2022a. fitlm and fitlme functions were used to complete the linear regression and mixed effects models, respectively.

Results

Figure 2 summarizes the results of the quality control and participant selection process. The baseline and longitudinal demographics and clinical characteristics of the PD patients included in this study are summarized in Table 2. Among all PD participants in the PPMI, our study focused on the subset of 546 individuals with idiopathic PD that had T1w MRI available at the initial visit, excluding genetic variants and SWEDD cases. A total of 445 PD patients had baseline MRI and clinical assessments available, with ages between 33.8 and 84.9. Additionally, 430 participants had longitudinal clinical assessments available, resulting in a final longitudinal dataset of 430 patients with 5068 timepoints. There were no significant differences in demographic and clinical characteristics of the included patients and those that were excluded based on MRI QC (Table S.1 in Supplementary Materials).

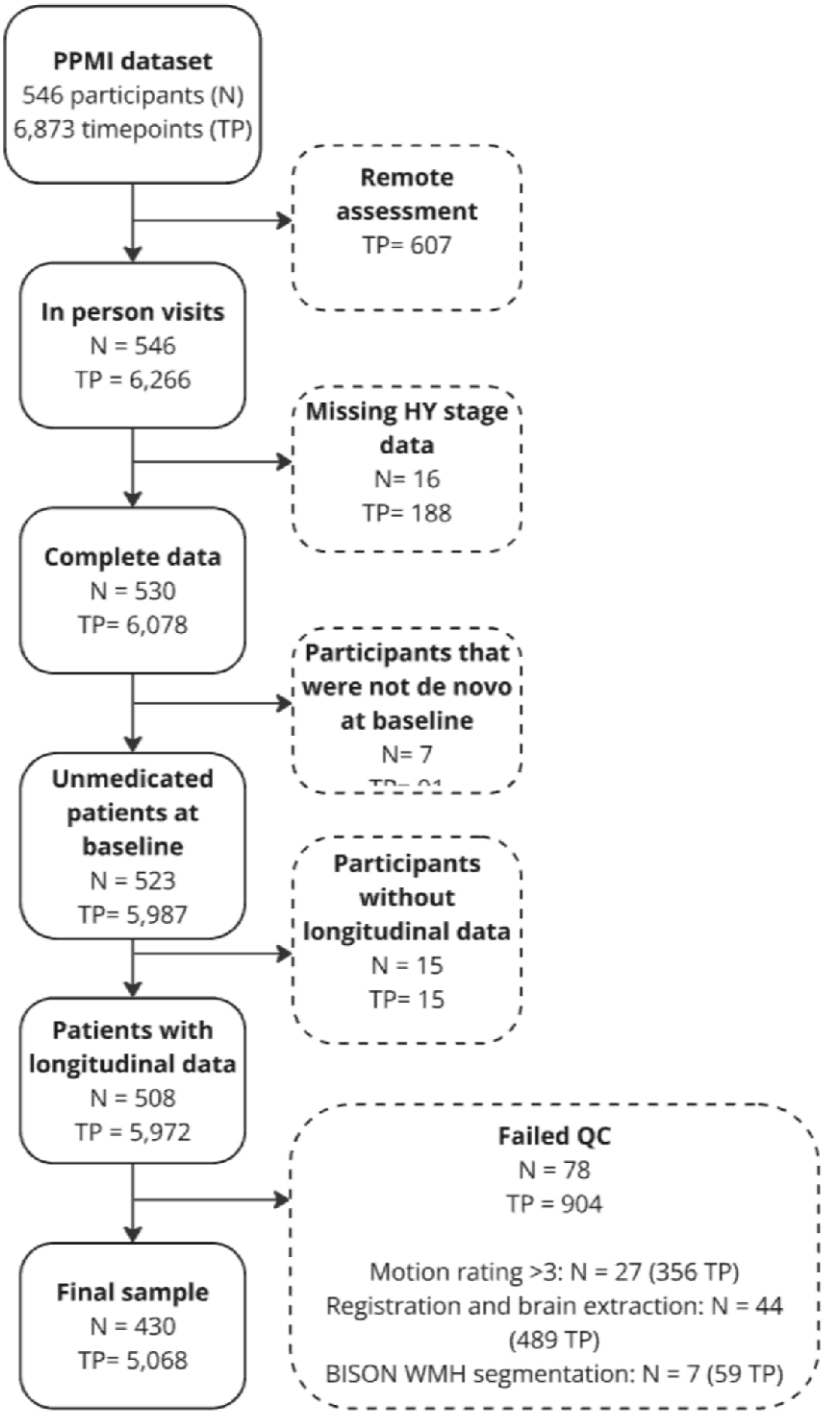

Figure 2. Diagram summarizing the participant selection procedure. A total of 116 participants were excluded due to unavailability of clinical assessments, presence of MRI artifacts, or failure of image processing steps, leading to a final sample of 430 de novo PD patients with 5,068 longitudinal clinical assessments. TP: Time point. QC: Quality control. HY: Hoehn and Yahr.

Table 2. Characteristics of the participants included in this study.

Measure	Baseline-only Sample	Longitudinal Sample at Baseline	Longitudinal Timepoints
N (Visit)	**445 (445)**	**430 (430)**	**430 (5068)**
Sex (%female)	150(33.7)	145(33.7)	1676 (33.07)
Age	62.42 ± 9.62	62.27 ± 9.63	64.38 ± 9.88
Years from Baseline	-	-	3.21 ± 3.1
Education Years	15.99 ± 2.99	16.01 ± 2.97	15.88 ± 2.85
MOCA	27.10 ± 2.26	27.01 ± 2.48	26.75 ± 3.03
LEDD	-	-	364.15 ± 388.41
Apathy Score	0.24 ± 0.57	0.23 ± 0.57	0.35 ± 0.68
GDS	2.30 ± 2.48	2.27 ± 2.47	2.60 ± 2.76
HY Stage	1.61 ± 0.50	1.62 ± 0.50	1.87 ± 0.55
UPDRS-III	21.41 ± 8.96	21.39 ± 9.09	25.94 ± 12.08

MoCA: Montreal Cognitive Assessment. LEDD: levodopa-equivalent daily dose. GDS: Geriatric Depression Scale. HY: Hoehn and Yahr. UPDRS: Unified Parkinson's Disease Rating Scale.

Hypothesis-based analyses

No cross-sectional regional associations survived multiple comparison corrections. The longitudinal hypothesis-based models revealed significant interaction effects between baseline atrophy (i.e., lower DBM values) and time in relation to apathy in the bilateral accumbens area, superior parietal, putamen, insula, left precuneus, right precentral, and cerebellum gray matter. (Fig. 3., Table S.2 in the supplementary materials).

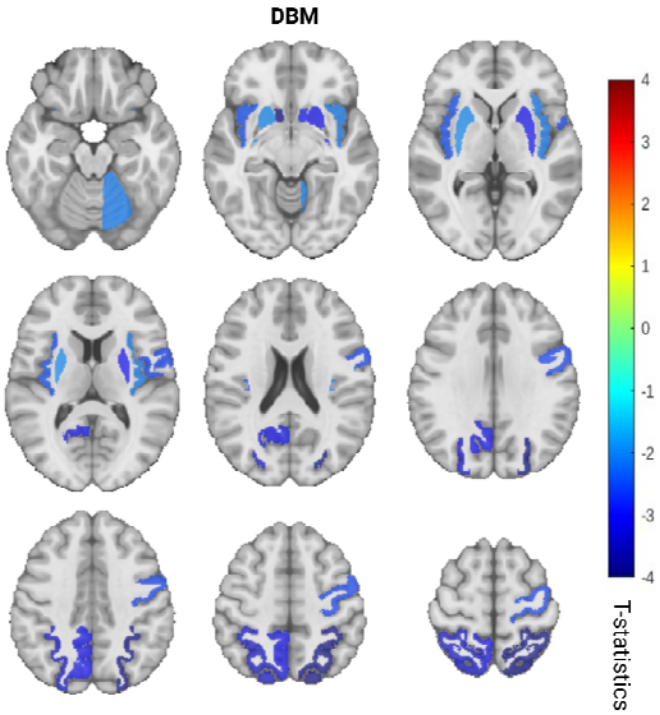

Figure 3. Longitudinal hypothesis-based analyses results. Cold colors indicate the t-statistics values corresponding to the significant longitudinal associations between regional atrophy and severity of future apathy.

Exploratory analyses

No cross-sectional regional associations survived multiple comparison corrections in the exploratory analyses for either DBM or WMH measurements. Longitudinal exploratory analyses further revealed significant interactions between baseline atrophy and time impacting future apathy in the bilateral lingual, parahippocampal, basal forebrain, ventral diencephalon, isthmus cingulate, thalamus, hippocampus, the left middle temporal, and right hemisphere, including the inferior temporal, peri calcarine, medial orbitofrontal, and cuneus. These results suggest that baseline atrophy in these regions may impact the longitudinal trajectory of apathy in PD (Fig.4.A, Table S.3 in the supplementary materials). Longitudinal assessment of WMHs also showed significant interactions of bilateral frontal lobe WMH burden at baseline and time impacting future apathy (Fig.4.B, Table S.4 in the supplementary materials).

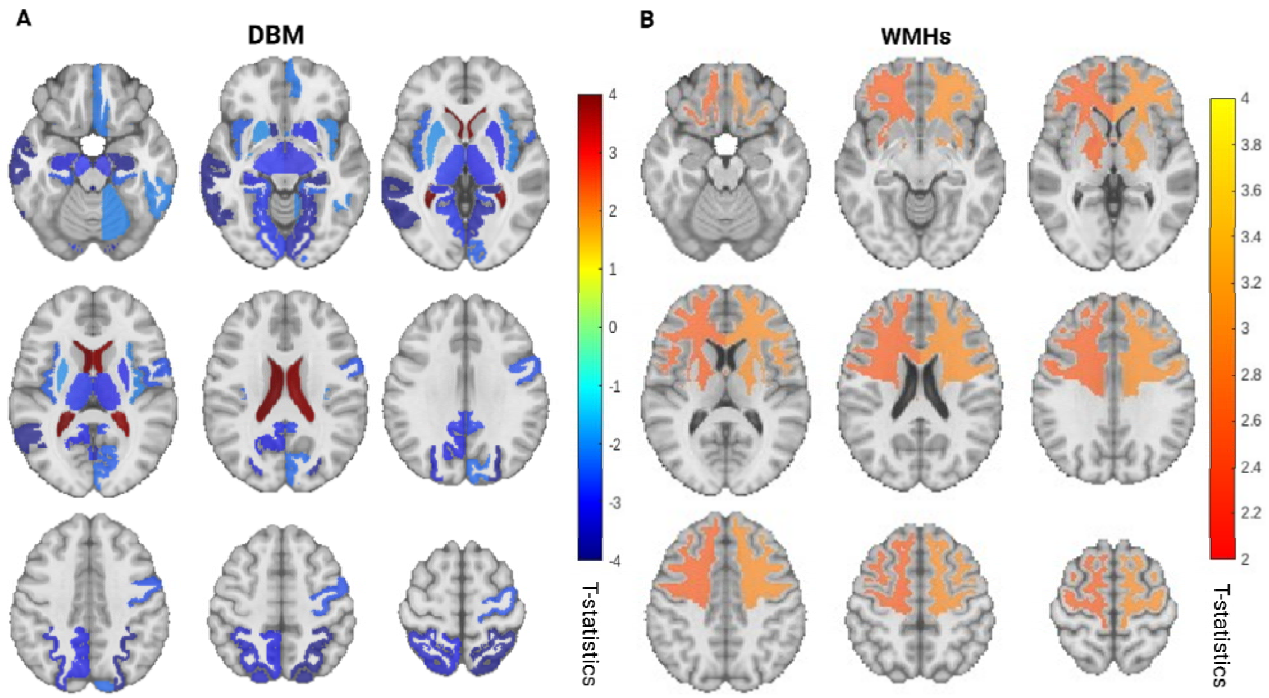

Figure 4. Longitudinal exploratory analysis results. A. Cold colors indicate the t-statistics values corresponding to the significant longitudinal associations between baseline regional atrophy and severity of future apathy. Warm colors indicate the significant longitudinal associations between baseline ventricular expansion and severity of future apathy. B. Colors indicate the t-statistics values corresponding to the significant longitudinal associations between baseline WMH burden and severity of future apathy.

Discussion

The present study investigated the underlying neural correlates of apathy in PD by utilizing a large dataset with longitudinal apathy assessments. Our findings emphasize the importance of specific brain regions in manifestation of apathy in de novo PD. Our cross-sectional analyses did not reveal any associations between apathy severity and regional atrophy at baseline when patients were at the de novo stage. Utilizing baseline DBM data and multiple apathy measurements per participant, our longitudinal mixed-effects modeling analyses confirmed significant associations between future apathy and baseline atrophy in the bilateral accumbens area[15,17,21], superior parietal[17], putamen[19], insula[14,16,19,23], left precuneus[14], precentral[14,16], and right cerebellum GM[20].

To further examine the relationship between brain structural changes and apathy severity, we conducted exploratory analyses using cross-sectional and longitudinal approaches. While we found no regions to show significant associations with apathy severity cross-sectionally, our longitudinal exploratory analysis revealed significant associations of atrophy in several regions with changes in apathy severity over time. This highlights the importance of considering disease progression in understanding the neural underpinnings of apathy in PD. The increased statistical power provided by our large sample size allowed us to extend previous findings in the literature

regarding the association between brain atrophy and apathy in PD. The absence of significant results in cross-sectional analyses suggests that the relationship between atrophy and apathy may be weak at baseline de novo stages and become more apparent with disease progression and therefore can be identified using a longitudinal framework. Our study revealed additional regions linked to apathy in PD, providing a more comprehensive understanding of the mechanisms underlying apathy in PD.

Associations between apathy and atrophy in regions such as the accumbens, putamen, insula, thalamus, and hippocampus suggest contributions to the motivational apathy subtype in this sample. This subtype is characterized by diminished reward sensitivity and reduced intrinsic motivation[6,11]. In addition, this interpretation is supported by atrophy in the parahippocampal, ventral diencephalon, and cingulate isthmus, implicating these regions in reward processing and emotional regulation[6,11]. It is worth noting that in areas related to functional impairment such as the medial frontal cortex, orbitofrontal cortex, and caudate nucleus, no significant relationship was found between the progression of apathy and atrophy [6]. This suggests that cognitive apathy, associated with executive dysfunction, is less prominent in this group of PD patients[6].

Utilizing quantitative volumetric assessments, we found that frontal lobe WMH burden at baseline is strongly associated with the increase in apathy scores over time. Our lobar WMH segmentation allows us to examine the correlation of WMH burden with apathy progression both at the whole brain level and within specific brain lobes. This approach provided a more precise understanding of brain changes associated with apathy, which was previously unexamined[30]. Our results suggest that early WMH burden at the frontal lobes is significantly associated with worsening apathy in the future. As WMHs can be managed (e.g. through antihypertensive medications), targeting vascular pathology early might offer a therapeutic avenue to mitigate the progression of apathy in PD patients[32]. This suggests the importance of incorporating WMH burden assessments in routine clinical evaluations to better predict and manage apathy in PD.

The image processing pipelines used in this study have been specifically developed and extensively validated for use in multi-center and multi-scanner applications, and have previously been employed in numerous studies to investigate atrophy and WMH burden in aging[55] and different neurodegenerative disorders such as Alzheimer's disease[45,56], frontotemporal dementia[57,58], amyotrophic lateral sclerosis[59,60], multiple sclerosis[61], and PD[62–65]. Further still, all image processing steps were quality controlled to ensure the accuracy of the derived atrophy and WMH measurements. Our study also has limitations that need to be taken into account. While the UPDRS-I is used in the PPMI dataset, its accuracy in assessing apathy is limited compared to other more comprehensive apathy assessment tools. In this regard, Pagonabarraga et al[11]. highlight that while the UPDRS-I is useful for screening purposes, it might lack the depth and specificity needed to assess apathy at PD. In contrast, scales such as the SAS and the LARS are more robust in assessing apathy as they investigate a more comprehensive set of dimensions of apathy, including motivation, emotional response, and goal-directed behavior. In addition, NPI is also more effective than UPDRS-I in capturing the multifaceted nature of apathy. Thus, future

research should consider integrating multiple apathy assessment tools and explore the onset and progression of neuropsychiatric symptoms in PD. Furthermore, the PPMI dataset does not include FLAIR images for all participants which would be optimal for WMH assessments. While our T1w-based WMH measurements have been shown to hold strong correlations with FLAIR-based WMHs ($r = 0.96$, $p < 0.001$), future studies should also assess the relationship between apathy and FLAIR-based WMHs, which would be better indicators of the extent of WM damage[44].

Conclusion

Our study highlights the relationships between regional brain atrophy and WMH burden and future apathy in PD, providing important insights into the neural basis of apathy. Recognizing the contribution of WMHs to future apathy in PD provides an opportunity for timely interventions, improving the quality of life in the patients.

Acknowledgements

Data used in this article were obtained from the Parkinson's Progression Markers Initiative (PPMI) database (www.ppmi-info.org/data). For up-to-date information on the study, visit www.ppmi-info.org. PPMI is sponsored and partially funded by the Michael J Fox Foundation for Parkinson's Research and funding partners, including AbbVie, Avid Radiopharmaceuticals, Biogen, Bristol-Myers Squibb, Covance, GE Healthcare, Genentech, GlaxoSmithKline (GSK), Eli Lilly and Company, Lundbeck, Merck, Meso Scale Discovery (MSD), Pfizer, Piramal Imaging, Roche, Servier, and UCB (www.ppmi-info.org/fundingpartners). The authors also acknowledge use of Compute Canada (https://alliancecan.ca/en) resources for performing the image processing analyses in the presented work.

Funding

RM and HA are supported by doctoral scholarships from Fonds de Recherche du Québec - Santé (FRQS). Dadar reports research funds from the Canadian Institutes of Health Research (CIHR), FRQS, Natural Sciences and Engineering Research Council of Canada (NSERC), Brain Canada, Healthy Brains for Healthy Lives (HBHL), and Douglas Research Centre (DRC). Zeighami reports research funds from the CIHR, NSERC, FRQS, and DRC.

References

1. Chambers LW, Chambers LW. *Prevalence and Monetary Costs of Dementia in Canada*. Miscellaneous Agency; 2016.

2. Schapira AH, Chaudhuri KR, Jenner P. Non-motor features of Parkinson disease. *Nat Rev Neurosci*. 2017;18(7):435-450.

3. Aarsland D, Brønnick K, Ehrt U, et al. Neuropsychiatric symptoms in patients with

Parkinson's disease and dementia: frequency, profile and associated caregiver stress. *J Neurol Neurosurg Psychiatry*. 2007;78(1):36-42.

4. Aarsland D, Marsh L, Schrag A. Neuropsychiatric symptoms in Parkinson's disease. *Mov Disord*. 2009;24(15):2175-2186. doi:10.1002/mds.22589

5. Yan H, Onoda K, Yamaguchi S. Gray matter volume changes in the apathetic elderly. *Front Hum Neurosci*. 2015;9:318.

6. De Waele S, Cras P, Crosiers D. Apathy in Parkinson's disease: defining the park apathy subtype. *Brain Sci*. 2022;12(7):923.

7. Béreau M, Van Waes V, Servant M, Magnin E, Tatu L, Anheim M. Apathy in Parkinson's disease: Clinical patterns and neurobiological basis. *Cells*. 2023;12(12):1599.

8. Borod JC, ed. *The Neuropsychology of Emotion*. Oxford University Press; 2000.

9. Kawagoe T, Onoda K, Yamaguchi S. Apathy and executive function in healthy elderly—resting state fMRI study. *Front Aging Neurosci*. 2017;9:124.

10. Yan H, Wu H, Cai Z, et al. The neural correlates of apathy in the context of aging and brain disorders: a meta-analysis of neuroimaging studies. *Front Aging Neurosci*. 2023;15:1181558. doi:10.3389/fnagi.2023.1181558

11. Pagonabarraga J, Kulisevsky J, Strafella AP, Krack P. Apathy in Parkinson's disease: clinical features, neural substrates, diagnosis, and treatment. *Lancet Neurol*. 2015;14(5):518-531. doi:10.1016/S1474-4422(15)00019-8

12. Santangelo G, Trojano L, Barone P, Errico D, Grossi D, Vitale C. Apathy in Parkinson's disease: diagnosis, neuropsychological correlates, pathophysiology and treatment. *Behav Neurol*. 2013;27(4):501-513.

13. Pont□Sunyer C, Hotter A, Gaig C, et al. The Onset of Nonmotor Symptoms in Parkinson's disease (The ONSET PD Study). *Mov Disord*. 2015;30(2):229-237. doi:10.1002/mds.26077

14. Reijnders JSAM, Scholtissen B, Weber WEJ, Aalten P, Verhey FRJ, Leentjens AFG. Neuroanatomical correlates of apathy in Parkinson's disease: A magnetic resonance imaging study using voxel□based morphometry. *Mov Disord*. 2010;25(14):2318-2325. doi:10.1002/mds.23268

15. Carriere N, Besson P, Dujardin K, et al. Apathy in Parkinson's disease is associated with nucleus accumbens atrophy: A magnetic resonance imaging shape analysis. *Mov Disord*. 2014;29(7):897-903. doi:10.1002/mds.25904

16. Alzahrani H, Antonini A, Venneri A. Apathy in Mild Parkinson's Disease: Neuropsychological and Neuroimaging Evidence. *J Park Dis*. 2016;6(4):821-832. doi:10.3233/JPD-160809

17. Martinez-Horta S, Sampedro F, Pagonabarraga J, et al. Non-demented Parkinson's disease patients with apathy show decreased grey matter volume in key executive and reward-related

nodes. *Brain Imaging Behav*. 2017;11(5):1334-1342. doi:10.1007/s11682-016-9607-5

18. Lucas□Jiménez O, Ojeda N, Peña J, et al. Apathy and brain alterations in Parkinson's disease: a multimodal imaging study. *Ann Clin Transl Neurol*. 2018;5(7):803-814. doi:10.1002/acn3.578

19. Ye BS, Jeon S, Yoon S, et al. Effects of dopaminergic depletion and brain atrophy on neuropsychiatric symptoms in de novo Parkinson's disease. *J Neurol Neurosurg Psychiatry*. 2018;89(2):197-204.

20. Prange S, Metereau E, Maillet A, et al. Early limbic microstructural alterations in apathy and depression in de novo Parkinson's disease. *Mov Disord*. 2019;34(11):1644-1654. doi:10.1002/mds.27793

21. Morris LA, Harrison SJ, Melzer TR, et al. Altered nucleus accumbens functional connectivity precedes apathy in Parkinson's disease. *Brain*. 2023;146(7):2739-2752. doi:10.1093/brain/awad113

22. Sampedro F, Puig-Davi A, Martinez-Horta S, et al. Cortical macro and microstructural correlates of cognitive and neuropsychiatric symptoms in Parkinson's disease. *Clin Neurol Neurosurg*. 2023;224:107531.

23. Rashidi□Ranjbar N, Churchill NW, Black SE, et al. Neuropsychiatric symptoms and brain morphology in patients with mild cognitive impairment, cerebrovascular disease and Parkinson disease: A cross sectional and longitudinal study. *Int J Geriatr Psychiatry*. 2024;39(3):e6074. doi:10.1002/gps.6074

24. Cummings JL, Mega M, Gray K, Rosenberg-Thompson S, Carusi DA, Gornbein J. The Neuropsychiatric Inventory: Comprehensive assessment of psychopathology in dementia. *Neurology*. 1994;44(12):2308-2308. doi:10.1212/WNL.44.12.2308

25. Sockeel P. The Lille apathy rating scale (LARS), a new instrument for detecting and quantifying apathy: validation in Parkinson's disease. *J Neurol Neurosurg Psychiatry*. 2006;77(5):579-584. doi:10.1136/jnnp.2005.075929

26. Reliability, validity, and clinical correlates of apathy in Parkinson's disease. *J Neuropsychiatry Clin Neurosci*. 1992;4(2):134-139. doi:10.1176/jnp.4.2.134

27. Marin RS, Biedrzycki RC, Firinciogullari S. Reliability and validity of the apathy evaluation scale. *Psychiatry Res*. 1991;38(2):143-162. doi:10.1016/0165-1781(91)90040-V

28. Grool AM, Geerlings MI, Sigurdsson S, et al. Structural MRI correlates of apathy symptoms in older persons without dementia: AGES-Reykjavik Study. *Neurology*. 2014;82(18):1628-1635. doi:10.1212/WNL.0000000000000378

29. Wen MC, Thiery A, Tseng WYI, et al. Apathy is associated with white matter network disruption and specific cognitive deficits in Parkinson's disease. *Psychol Med*. 2022;52(2):264-273.

30. Zhang Y, Zhang GY, Zhang ZE, He AQ, Gan J, Liu Z. White matter hyperintensities: a

marker for apathy in Parkinson's disease without dementia? *Ann Clin Transl Neurol*. 2020;7(9):1692-1701. doi:10.1002/acn3.51159

31. Misquitta K, Dadar M, Louis Collins D, Tartaglia MC. White matter hyperintensities and neuropsychiatric symptoms in mild cognitive impairment and Alzheimer's disease. *NeuroImage Clin*. 2020;28:102367. doi:10.1016/j.nicl.2020.102367

32. Dadar M, Zeighami Y, Yau Y, et al. White matter hyperintensities are linked to future cognitive decline in de novo Parkinson's disease patients. *NeuroImage Clin*. 2018;20:892-900. doi:10.1016/j.nicl.2018.09.025

33. Dadar M, Mahmoud S, Zhernovaia M, Camicioli R, Maranzano J, Duchesne S. White matter hyperintensity distribution differences in aging and neurodegenerative disease cohorts. *NeuroImage Clin*. 2022;36:103204. doi:10.1016/j.nicl.2022.103204

34. Fazekas F, Chawluk J, Alavi A, Hurtig H, Zimmerman R. MR signal abnormalities at 1.5 T in Alzheimer's dementia and normal aging. *Am J Roentgenol*. 1987;149(2):351-356. doi:10.2214/ajr.149.2.351

35. Marek K, Chowdhury S, Siderowf A, et al. The Parkinson's progression markers initiative (PPMI) – establishing a PD biomarker cohort. *Ann Clin Transl Neurol*. 2018;5(12):1460-1477. doi:10.1002/acn3.644

36. Goetz CG, Tilley BC, Shaftman SR, et al. Movement Disorder Society□sponsored revision of the Unified Parkinson's Disease Rating Scale (MDS□UPDRS): Scale presentation and clinimetric testing results. *Mov Disord*. 2008;23(15):2129-2170. doi:10.1002/mds.22340

37. Coupé, P., Yger, P., Prima, S., Hellier, P., Kervrann, C., & Barillot, C. (2008). An optimized blockwise nonlocal means denoising filter for 3-D magnetic resonance images. *IEEE transactions on medical imaging*, *27*(4), 425-441.

38. Sled, J. G., Zijdenbos, A. P., & Evans, A. C. (1998). A nonparametric method for automatic correction of intensity nonuniformity in MRI data. *IEEE transactions on medical imaging*, *17*(1), 87-97.

39. Dadar, M., Fonov, V. S., Collins, D. L., & Alzheimer's Disease Neuroimaging Initiative. (2018). A comparison of publicly available linear MRI stereotaxic registration techniques. *Neuroimage*, *174*, 191-200.

40. Avants, B. B., Epstein, C. L., Grossman, M., & Gee, J. C. (2008). Symmetric diffeomorphic image registration with cross-correlation: evaluating automated labeling of elderly and neurodegenerative brain. *Medical image analysis*, *12*(1), 26-41.

41. Manera, A. L., Dadar, M., Fonov, V., & Collins, D. L. (2020). CerebrA, registration and manual label correction of Mindboggle-101 atlas for MNI-ICBM152 template. *Scientific Data*, *7*(1), 237.

42. Ashburner J, Friston KJ. Voxel-based morphometry—the methods. *Neuroimage*. 2000;11(6):805-821.

43. Dadar M, Collins DL. BISON: Brain tissue segmentation pipeline using T_1 weighted magnetic resonance images and a random forest classifier. *Magn Reson Med*. 2021;85(4):1881-1894. doi:10.1002/mrm.28547

44. Dadar M, Maranzano J, Ducharme S, et al. Validation of T 1w based segmentations of white matter hyperintensity volumes in large scale datasets of aging. *Hum Brain Mapp*. 2018;39(3):1093-1107. doi:10.1002/hbm.23894

45. Kamal F, Morrison C, Maranzano J, Zeighami Y, Dadar M. White Matter Hyperintensity Trajectories in Patients With Progressive and Stable Mild Cognitive Impairment. *Neurology*. 2023;101(8). doi:10.1212/WNL.0000000000207514

46. Dadar M, Miyasaki J, Duchesne S, Camicioli R. White matter hyperintensities mediate the impact of amyloid ß on future freezing of gait in Parkinson's disease. *Parkinsonism Relat Disord*. 2021;85:95-101. doi:10.1016/j.parkreldis.2021.02.031

47. Morrison C, Dadar M, Manera AL, Collins DL. Racial differences in white matter hyperintensity burden in older adults. *Neurobiol Aging*. 2023;122:112-119. doi:10.1016/j.neurobiolaging.2022.11.012

48. Dadar M. Hammers Atlas Registered to ICBM. Published online May 12, 2023. doi:10.5281/ZENODO.7930159

49. Dadar M, Maranzano J, Misquitta K, et al. Performance comparison of 10 different classification techniques in segmenting white matter hyperintensities in aging. *NeuroImage*. 2017;157:233-249.

50. Pardoe, H. R., Hiess, R. K., & Kuzniecky, R. (2016). Motion and morphometry in clinical and nonclinical populations. *Neuroimage*, *135*, 177-185.

51. Savalia, N. K., Agres, P. F., Chan, M. Y., Feczko, E. J., Kennedy, K. M., & Wig, G. S. (2017). Motion related artifacts in structural brain images revealed with independent estimates of in scanner head motion. *Human brain mapping*, *38*(1), 472-492.

52. Moqadam R, Dadar M, Zeighami Y. Investigating the impact of motion in the scanner on brain age predictions. *Imaging Neurosci*. 2024;2:1-21.

53. Brzezinski-Rittner A, Moqadam R, Iturria-Medina Y, Chakravarty MM, Dadar M, Zeighami Y. Disentangling the effect of sex from brain size on brain organization and cognitive functioning. *GeroScience*. 2025. doi:10.1007/s11357-024-01486-5

54. Benjamini Y, Hochberg Y. Controlling the False Discovery Rate: A Practical and Powerful Approach to Multiple Testing. *J R Stat Soc Ser B Stat Methodol*. 1995;57(1):289-300. doi:10.1111/j.2517-6161.1995.tb02031.x

55. Morrison C, Dadar M, Villeneuve S, Collins DL. White matter lesions may be an early marker for age-related cognitive decline. *NeuroImage Clin*. 2022;35:103096. doi:10.1016/j.nicl.2022.103096

56. Kamal F, Morrison C, Maranzano J, Zeighami Y, Dadar M. Topographical differences in

white matter hyperintensity burden and cognition in aging, MCI, and AD. *GeroScience*. 2023;45(1):1-16. doi:10.1007/s11357-022-00665-6

57. Metz A, Zeighami Y, Ducharme S, Villeneuve S, Dadar M. Frontotemporal Dementia Subtyping using Machine Learning, Multivariate Statistics, and Neuroimaging. *Brain Commun*. 2025.

58. Dadar M, Manera AL, Ducharme S, Collins DL. White matter hyperintensities are associated with grey matter atrophy and cognitive decline in Alzheimer's disease and frontotemporal dementia. *Neurobiol Aging*. 2022;111:54-63. doi:10.1016/j.neurobiolaging.2021.11.007

59. Lajoie I, Canadian ALS Neuroimaging Consortium (CALSNIC), Kalra S, Dadar M. Regional cerebral atrophy contributes to personalized survival prediction in ALS: a multicentre, machine learning, deformation based morphometry study. *Annals of Neurology*. 2025.

60. Dadar M, Manera AL, Zinman L, et al. Cerebral atrophy in amyotrophic lateral sclerosis parallels the pathological distribution of TDP43. *Brain Commun*. 2020;2(2):fcaa061. doi:10.1093/braincomms/fcaa061

61. Dadar M, Narayanan S, Arnold DL, Collins DL, Maranzano J. Conversion of diffusely abnormal white matter to focal lesions is linked to progression in secondary progressive multiple sclerosis. *Mult Scler J*. 2021;27(2):208-219. doi:10.1177/1352458520912172

62. Zeighami Y, Ulla M, Iturria-Medina Y, et al. Network structure of brain atrophy in de novo Parkinson's disease. *eLife*. 2015;4:e08440. doi:10.7554/eLife.08440

63. Yau Y, Zeighami Y, Baker TE, et al. Network connectivity determines cortical thinning in early Parkinson's disease progression. *Nat Commun*. 2018;9(1):12. doi:10.1038/s41467-017-02416-0

64. Pandya S, Zeighami Y, Freeze B, et al. Predictive model of spread of Parkinson's pathology using network diffusion. *NeuroImage*. 2019;192:178-194. doi:10.1016/j.neuroimage.2019.03.001

65. Dagher A, Zeighami Y. Testing the Protein Propagation Hypothesis of Parkinson Disease. *J Exp Neurosci*. 2018;12:1179069518786715. doi:10.1177/1179069518786715

Supplementary Materials

Table S.1. Comparison of the demographics and clinical variables between the participants included and excluded in the study

Variable	**Excluded**	**Included**	**P Value**
Age	63.317 ± 10.093	62.177 ± 9.635	0.3
Sex	1.667 ± 0.475	1.661 ± 0.474	0.93
Education_Years	16.000 ± 3.379	15.979 ± 2.992	0.997
MOCA	26.556 ± 2.926	27.110 ± 2.271	0.296
GDS	1.789 ± 2.261	2.268 ± 2.462	0.045
Apathy Score	0.099 ± 0.300	0.233 ± 0.563	0.079
HY Stage	1.618 ± 0.490	1.613 ± 0.501	0.913
UPDRS III	22.099 ± 8.469	21.394 ± 9.003	0.361

Table S.2. Hypothesis-based results for the longitudinal DBM analyses.

Hemisphere	**Left**				**Right**			
Region Names	ID	T stats	P values	P_{FDR}	ID	T stats	P values	P_{FDR}
Middle Frontal Gyrus	52	0.050	0.960	0.993	1	-1.004	0.316	0.451
Nucleus Accumbens	**55**	**-4.406**	**<0.001**	**<0.001**	**4**	**-3.305**	**0.001**	**0.005**
Orbitofrontal Cortex	58	-2.101	0.036	0.082	7	-2.285	0.022	0.056
Rostral Anterior Cingulate	59	-0.880	0.379	0.516	8	0.432	0.666	0.799
Superior Parietal Gyrus	**60**	**-3.831**	**<0.001**	**0.001**	**9**	**-4.385**	**<0.001**	**<0.001**
Inferior Parietal Gyrus	61	-1.410	0.159	0.280	10	0.351	0.726	0.838
Putamen	**72**	**-2.374**	**0.018**	**0.048**	**21**	**-3.435**	**0.001**	**0.004**
Insula	**74**	**-2.891**	**0.004**	**0.014**	**23**	**-2.540**	**0.011**	**0.037**
Precuneus	**82**	**-3.478**	**0.001**	**0.004**	31	-1.513	0.130	0.245
Precentral Gyrus	86	-0.098	0.922	0.988	**35**	**-3.032**	**0.002**	**0.010**
Caudal Midbrain	93	-0.610	0.542	0.678	42	-0.625	0.532	0.678
Inferior Frontal Gyrus	95	1.964	0.050	0.106	44	1.349	0.177	0.296
Superior Temporal Gyrus	96	-1.250	0.211	0.317	45	-1.256	0.209	0.317
cerebellum gray matter	97	-1.673	0.094	0.189	**46**	**-2.494**	**0.013**	**0.038**
Caudate	100	0.306	0.759	0.844	49	0.008	0.994	0.994

Table S.3. Exploratory results for the longitudinal DBM analyses.

Right Hemisphere				**Left Hemisphere**			
Region Names	ID	T stats	P_{FDR}	Region Names	ID	T stats	P_{FDR}
Inferior temporal	3	-2.5139	0.0382	Accumbens Area	55	-4.4058	<0.001
Accumbens Area	4	-3.3049	0.0051	Superior Parietal	60	-3.8314	0.0013
Pericalcarine	6	-2.8933	0.0146	Lingual	63	-3.2757	0.0053
Superior Parietal	9	-4.3848	<0.001	Para hippocampal	69	-3.0439	0.01
Lingual	12	-4.113	<0.001	Putamen	72	-2.374	0.05
Medial Orbitofrontal	15	-2.6134	0.0306	Insula	74	-2.8908	0.0146
Para hippocampal	18	-2.8694	0.015	Basal Forebrain	76	-5.0842	0
Putamen	21	-3.4351	0.0041	Ventral Diencephalon	77	-3.3631	0.0047
Insula	23	-2.5401	0.0366	Middle Temporal	79	-4.9283	0
Basal Forebrain	25	-5.3788	0	Precuneus	82	-3.4779	0.0037
Ventral Diencephalon	26	-3.6484	0.0025	Isthmus Cingulate	84	-3.359	0.0047
Isthmus Cingulate	33	-3.1874	0.0067	Fourth Ventricle	88	-3.895	0.0011
Precentral	35	-3.0322	0.01	Thalamus	91	-3.2696	0.0053
Fourth Ventricle	37	-4.001	<0.001	Lateral Ventricle	92	3.3309	0.0049
Thalamus	40	-3.478	0.0037	Hippocampus	99	-3.5901	0.0028
Lateral Ventricle	41	3.0832	0.0091				
Cuneus	43	-2.788	0.0187				
Cerebellum Gray Matter	46	-2.4936	0.0392				
Hippocampus	48	-4.3271	<0.001				

Table S.4. Exploratory results for the longitudinal WMH analyses.

Hemisphere	**Left**		**Right**	
Region Names	T stats	P_{FDR}	T stats	P_{FDR}
Frontal Lobe	**2.560**	**0.047**	**2.950**	**0.029**
Temporal Lobe	1.641	0.182	2.022	0.097

Parietal Lobe	0.172	0.864	0.282	0.864
Occipital Lobe	-0.839	0.516	-1.538	0.186